Modeling water needs and total irrigation depths of maize crop in the south west of France using high spatial and temporal resolution satellite imagery

Marjorie Battude, Ahmad Al Bitar, Aurore Brut, Tiphaine Tallec, Mireille Huc, Jérôme Cros, Jean-Jacques Weber, Ludovic Lhuissier, Vincent Simonneaux, Valérie Demarez

Modeling water needs and total irrigation depths of maize crop in the south west of France using high spatial and temporal resolution satellite imagery

Marjorie Battude[1*], Ahmad Al Bitar[1], Aurore Brut[1], Tiphaine Tallec[1], Mireille Huc[1], Jérôme Cros[1], Jean-Jacques Weber[2], Ludovic Lhuissier[2], Vincent Simonneaux[1], Valérie Demarez[1]

[1] CESBIO, Université de Toulouse, CNES/CNRS/IRD/UPS, Toulouse, France

[2] Compagnie d'Aménagement des Coteaux de Gascogne (CACG), Tarbes, France

****** Corresponding author: marjorie.battude@cesbio.cnes.fr***

Centre d'Etudes Spatiales de la BIOsphère

Address: CESBIO, 18 Avenue Edouard Belin, 31401 Toulouse Cedex 4, France

Tel: (33) 5 61 55 85 78

Keywords

Evapotranspiration

Irrigation management

Crop Model

Maize

Remote sensing

ABSTRACT

Climate change is projected to increase water resources limitation and to impact significantly agricultural production. A big challenge for agriculture will be to reduce the amount of water used to fit the environmental constraints, while maintaining a level of production that ensure food security. In this context, we propose a methodology based on high spatial and temporal resolution remote sensing data combined with a semi-empirical crop model coupling the Simple Algorithm For Yield estimates (SAFY, Duchemin et al., 2008, 2015; Battude et al., 2016) and a water balance model adapted from the FAO-56 method (Allen et al., 1998). A module was added to automatically simulate irrigation. The model was used to assess the dynamics of actual Evapotranspiration (ETca) and water supplies of maize crop over large areas and during contrasted climatic years in the south west of France. The model was first calibrated and evaluated over an experimental field using four years of ETca measurements. The validation was done over 18 maize fields and larger irrigated zones (135 ha to 450 ha) using total irrigation depths. This work permitted to quantify the ability of different methods to estimate the storage capacity (soil map vs *in situ* data) and the basal crop coefficient Kcb (standard vs remotely sensed values) and their impact on total irrigation depths. Good estimations were obtained for ETca (R = 0.88; RRMSE = 20%). The model also reproduced correctly the total irrigation depth over the 18 maize fields (R = 0.79; RRMSE = 18.8%) and three larger irrigated zones (R = 0.8; RRMSE = 42%). The underestimation (Bias = -93 mm) may be due to different reasons such as errors in soil water storage capacity estimates, but also to an overestimation of water needs by water managers or a potential over-irrigation carried out by farmers. Finally, the work demonstrates the high potential of combining a simple agro-meteorological model using only few parameters with satellite imagery for a large-scale monitoring of total irrigation depth.

1. INTRODUCTION

Agriculture is by far the main consumer of fresh water with about 70% of all withdrawals devoted to irrigation (UNESCO, 2015). With the multiplication of extreme weather events, irrigation has become essential to ensure a reliable, stable and profitable production. In a world where population is constantly increasing and with high climate extremes, a big challenge for agriculture will be to maintain a sufficient level of crop production while reducing the amount of water used, and therefore to increase its use efficiency (Kijne et al., 2003). Indeed, an important amount of water allotted to irrigation is not efficiently used by crop (Smith et al., 1992). This naturally leads the scientific community to work on management tools to both ensure food security and meet environmental issues.

The present study was conducted in the south west of France on irrigated maize fields. In this region, maize crop (*Zea mays*) represents 60% of irrigated lands, consuming 70 to 80% of whole irrigation water (around 250.10^6 m^3/year).

Several agronomical crop models are developed to assess specific agronomical needs like grain yield or irrigation demand prediction (e.g. DSSAT (Jones et al., 2003), STICS (Brisson et al., 2003)). However, if such crop models are quite suitable for monitoring plant development at the field scale, their implementation over larger areas is often limited by the availability of input data. To overcome these difficulties, a widely used solution is to integrate satellite observations into semi-empirical crop models (see Dorigo et al., 2007 for review). Halfway between complex and empirical approaches, these models combine the descriptions of the main biophysical processes and simple empirical parameterizations (e.g., AquaCrop (Steduto et al., 2009), AqYield (Constantin et al., 2015), GRAMI (Maas, 1992), Pilote (Mailhol et al., 1997), PolyCrop (Nana et al., 2014), SAFY (Duchemin et al., 2008; Battude et al., 2016)).

This approach combining remote sensing data and crop models has been made possible by the development of new sensors providing high resolution images, necessary to an accurate vegetation

monitoring, and has been particularly popular for the monitoring of water resources and irrigation water supplies at the regional scale (Duchemin et al., 2006; Zwart et al., 2010; Droogers et al., 2010; Saadi et al., 2015; Toureiro et al., 2016). Most of the models among the previously cited studies did not allow to estimate both the water needs and supplies, the biomass production and yields. In a previous study, Battude et al. (2016) proposed a remote sensing driven approach to estimate the maize biomass production and yield for both irrigated and rainfed fields. An original methodology was developed specifically for large areas with a limited use of *in situ* information. In that purpose, we used a quite simple semi-empirical model, the SAFY (i.e. Simple Algorithm For Yield estimates) model (Duchemin et al., 2008) driven by high spatial and temporal resolution images, which is able to take into account the dynamic of vegetation without requiring information about soil characteristics. This last study led to a new formalism of the Effective Light Use Efficiency (*ELUE*) and the Specific Leaf Area (*SLA*) that was implemented in the original version of the SAFY model. Results revealed that the new version of the model improves yield estimates both at field scale (RRMSE = 13.7%) and at regional scale (RRMSE = 5%). However, this new version of the model did not include a water balance module and, thus, did not give access to the crop water needs and supplies which knowledge is essential in a context of water management. The original version of the SAFY model had already been coupled with FAO methods on rainfed wheat crops (Duchemin et al., 2015) and had led to good estimates of biomass, ETca and soil water content. We thus coupled the new version of the SAFY model with the FAO-56 method and a sub-module simulating irrigation in which irrigation events are triggered according to the water stress level of the crop, in order to simulate both biomass production and water needs and supplies.

Even though the FAO-56 methods are sometimes questioned, they remain the most commonly approach used for the estimation of crop evapotranspiration from field to global scales (Pereira et al., 2015) due to their relative simplicity. Indeed, the method allows estimating optimal crop Evapotranspiration (*ETc*) with a crop coefficient (*Kc*) applied to the reference evapotranspiration (ET_0).

Such approach overcomes the difficulties encountered with direct measurements (e.g. *Eddy-Covariance, Bowen ratio energy balance, lysimeters*) for which applications are restrained to field scale because of the heavy and costly needed investment. The accurate estimation of actual crop Evapotranspiration (*ETca*) over large areas is essential to improve water resource management. Given their strong impact on ETca, the crop coefficient and the plant water availability must be correctly estimated which is one of the major difficulties of the application of the FAO approach over large areas. Indeed, the standard crop coefficient method based on tabulated values implies "standard conditions" that do not vary from field to field and that are not actual most of the time. As crop characteristics correlate well with spectral reflectances, numerous studies aimed at developing empirical relationships between Kc and remote sensing data that allowed improving ETca estimates and irrigation scheduling (Bausch et al., 1987; Neale et al., 1989; Hunsaker et al., 2003; Glenn et al., 2011).

Beside the importance of an accurate estimation of Kc, the knowledge of the Storage Capacity (*SC*) of the soil is also useful as it is a widely used concept for a large panel of models. This integrative value relies on the knowledge of soil properties that are rarely available over large areas. Moreover, some sensitivity analyses have demonstrated the large impact of uncertainty of the SC values on yield estimates (Pachepsky and Acock, 1998; Lawless et al., 2008) or on the soil hydraulic characteristics (Baroni et al., 2010).

The objectives of this study were twofold. First, we aimed at reproducing the seasonal dynamics of ETca and total irrigation depth over large areas and various contrasted climatic years. For that, we used a water balance crop model combined with high spatial and temporal resolution remote sensing data. Second, we aimed at evaluating the impact on simulated ETca and total irrigation depths of various methods used to determine the soil water storage capacity (SC) and the crop coefficient (Kc).

2. MATERIAL & METHODS

2.1. Model description

In this study, we used the SAFY-FAO model. This model combines the SAFY crop model (Duchemin et al., 2008; Battude et al., 2016) with a water balance model proposed by the FAO-56 method (Allen et al., 1998) and a sub-module simulating irrigation events, hereafter referred to as "automatic irrigation module". The SAFY-FAO model simulates the dynamics of Green Area Index (*GAI* in $m^2.m^{-2}$, ratio of the photosynthetically active plant area, without organ distinction, per meter square ground; Baret et al., 2010), Dry Aboveground Mass (*DAM* in $g.m^{-2}$), actual crop Evapotranspiration (*ETca* in $mm.day^{-1}$) and Current Available Water (*CAW* in mm) in three soil layers (i.e. top, intermediate and deep) at a daily time step from a date of plant emergence (D_0). It can be run in two different ways: using the real irrigation supplies (forced mode) or activating the automatic irrigation module (automatic mode). Remotely sensed GAI and green cover fraction (*FCOVER*), incoming global radiation (*Rg* in $MJ.m^{-2}$), air temperature (*Ta* in °C), reference evapotranspiration (ET_0 in $mm.day^{-1}$), precipitation and irrigation (in the forced mode case) are used as inputs. ET_0 is derived from climatic parameters according to the Penman-Monteith equation recommended by FAO (Allen et al., 1998), which is adapted for a hypothetical grass reference surface.

The GAI (in $m^2.m^{-2}$) is simulated by the SAFY crop model (Duchemin et al., 2008). In the present study, we used the new formulation of vegetation dynamics proposed in Battude et al. (2016). This new version of the SAFY model includes sixteen parameters (*Table 1*) allowing the seasonal variation of the Specific Leaf Area (SLA in m2.g-1) and the Effective Light Use Efficiency (ELUE in g.MJ-1) (see Battude et al., 2016 for details). The SLA is defined as the ratio of leaf area to dry mass and it allows converting daily leaf mass production into daily leaf area growth. The SLA increase with time is due to the increasing leaves thickness during the plant growth. The ELUE corresponds to the plant efficiency to

convert radiation into aboveground biomass. The rise of ELUE during the plant growth may be due to several processes, among them the variation of the root-shoot ratio (Amos and Walters, 2006). The biomass production (Δ_{DAM}, [Eq. 1]) is based on the Monteith's light-use efficiency theory (Monteith, 1972). It depends on the effective light-use efficiency (*ELUE*), on a stress factor (F_T) being function of the daily air temperature (*Ta*) and on the daily photosynthetically active radiation absorbed by canopy (*APAR* in MJ.m^{-2}), and is limited by the water stress coefficient (*Ks*). The Ks ([Eq. 2]) daily value varies from 0 (complete stress) to 1 (no stress) and depends on a critical humidity parameter (*Dft,* for "Transpiration reduction coefficient") and on the soil maximal relative humidity (*RHtot*). The RHtot ([Eq. 3]) depends on the relative humidity of the two first layers (RH_1 and RH_2), those in which the roots develop. The relative humidity of a soil layer (RH_x, [Eq. 4]) corresponds to the ratio between the current available water in the soil layer (*CAW* in mm) and its water storage capacity (*SC* in mm). SC ([Eq. 5]) depends on the soil layer thickness (SLT_x in mm) and on the water content at field capacity (H_{fc} in m^3.m^{-3}) and at wilting point (H_{wp} in m^3.m^{-3}). The SLT of the intermediate layer (SLT_2 in mm) increases with the root depth (*RD* in mm, [Eq. 6]), constrained by the soil maximal depth (*SD* in mm) and depending on the air temperature (*Ta* in °C), the minimal temperature for growth (*Tmin* in °C), the Ks coefficient and the root growth rate (*Vpr* in mm.°C).

$$\Delta_{DAM} = ELUE * F_T(Ta) * Ks * APAR \quad \text{[Eq. 1]}$$

$$Ks = \min\left\{1 - \frac{RHtot - Dft}{-Dft}, 1\right\} \quad \text{[Eq. 2]}$$

$$RHtot = max\{RH_1, RH_2\} \quad \text{[Eq. 3]}$$

$$RH_x = CAW_x / SC_x \quad \text{[Eq. 4]}$$

$$SC_x = \left(H_{fc} - H_{wp}\right) * SLT_x \quad \text{[Eq. 5]}$$

$$RD_{(j)} = min\{RD_{(j-1)} + max\{Ta - Tmin, 0\} * Ks * Vpr, SD * 0.9\} \quad \text{[Eq. 6]}$$

The water balance model includes nine parameters that can be related to soil characteristics (H_{fc}, H_{wp}, *SD*, SLT_1, *β*) or vegetation characteristics (*Vpr*, Kcb_{max}, E_{trp}, *Dft*) (*Table 1*). Only vertical water

transfers are taken into account and surface runoff is neglected. ETca calculation is based on the dual-crop coefficient FAO-56 method, splitting the Kc parameter into *Ke* (i.e. soil water evaporation coefficient) and *Kcb* (i.e. basal crop coefficient) [Eq. 7 and Eq. 9] (Allen et al., 1998), the Ks being as defined previously. Soil evaporation (*E*, [Eq. 7]) depends on the reference evapotranspiration (ET_0) and on the Ke coefficient. The Ke ([Eq. 8]) is function of the green cover fraction (*FCOVER*), the top soil layer relative humidity (RH_1) and limited by a β function. Unlike Duchemin et al. (2015), the FCOVER, useful for the calculation of evaporation [Eq. 8], is estimated with the BVNet tool (see section 2.5. "Remote sensing GAI and FCOVER"). Plant transpiration (*T*, [Eq. 9]) depends on the Kcb, the ET_0 and the Ks as defined previously. The Kcb ([Eq. 10]) involved in the transpiration process is related to the GAI; the Kcb_{max} corresponding to the maximal transpiration coefficient and the *Etrp* being the exponent of the transpiration. Soil evaporation (*E*) is calculated according to the relative humidity of the top soil layer (RH_1) [Eq. 7 and Eq. 8], whereas both top and intermediate layers are used for the computation of the plant transpiration (*T*) [Eq. 9, Eq. 2 and Eq. 3]. Soil diffusive fluxes are simulated with [Eq. 11].

$$E = ET_0 * Ke \quad \text{[Eq. 7]}$$

$$Ke = (1 - FCOVER) * \left(1 - (1 - RH_1)^{\beta}\right) \quad \text{[Eq. 8]}$$

$$T = ET_0 * Kcb * Ks \quad \text{[Eq. 9]}$$

$$Kcb = Kcb_{max}\,(1 - e^{-E_{trp} * GAI}) \quad \text{[Eq. 10]}$$

$$\Phi_{xy} = K_{dif} * \left(\frac{H_x - H_y}{H_{fc}}\right)^{E_{dif}} \quad \text{[Eq. 11]}$$

When activated, the automatic irrigation module triggers an irrigation event at a fixed depth determined by the D_I parameter, when the Ks coefficient is lower than 1. This happens when the relative humidity (*RHtot*) reaches a defined threshold (*Dft*) [Eq. 2]. The simulated irrigation is then used as an input into the SAFY-FAO model. The period when irrigation can be triggered ranges from the plant emergence until the beginning of the senescence phase (i.e. *when the sum of temperature reaches a growing degree day threshold called* S_{TT}, in °C). After that day, irrigations are allowed only if the time

before harvest is higher than a specific number of days defined by I_{end} parameter.

	Name	Notation	Unit	Value	Data Sources
SAFY MODEL PARAMETERS	Climatic efficiency	ε_c	-	0.48	Literature (Varlet Grancher et al., 1982)
	Temperature for growth	T_{min}, T_{opt}, T_{max}	°C	8-30-45	Literature (Drouet and Pages, 2003)
	Polynomial degree	β_0	-	2	Literature (Drouet and Pages, 2003)
	Light-interception coefficient	K_{ext}	-	0.65	Literature (Cavero et al., 2000)
	Harvest index	HI	-	0.5	Literature (Steduto et al., 2012)
	Initial specific leaf area	SLA_0	$m^2.g^{-1}$	[0.024 ; 0.032]	Optimized using GAI (Battude et al., 2016)
	Leaf thickness coefficient	LTC	-	[-1.3e-05 ; -9e-06]	Optimized using GAI (Battude et al., 2016)
	Potential effective light-use efficiency	$ELUE_p$	$g.MJ^{-1}$	[7 ; 11]	Optimized using GAI (Battude et al., 2016)
	Plant maturation index	PMI	-	[-260 ; -300]	Optimized using GAI (Battude et al., 2016)
	Day of plant emergence	D_0	day of year	L1 +/20j	Logistic function (Battude et al., 2016)
	Sum of temperature for senescence	S_{TT}	°C	SMT(L3 +/20j)	Logistic function (Battude et al., 2016)
	Partition-to-leaf function : par a	Pl_a	-	[0.05 - 0.5]	Literature (Claverie et al., 2012)

	Partition-to-leaf function : par b	Pl_b	-	-	linked to Pl_a (Battude et al., 2016)
	Rate of senescence	RS	°C.day^{-1}	-	linked to S_{TT} (Battude et al., 2016)
SOIL	Soil top layer thickness	SLT_1	m	0.1	Literature (FAO-56 Allen et al., 1998)
	Soil maximal depth	SD	m	Measured	Measurements or Soil Map
	Humidity at field capacity	H_{fc}	$m^3.m^{-3}$	Measured	Measurements or Soil Map
	Humidity at wilting point	H_{wp}	$m^3.m^{-3}$	Measured	Measurements or Soil Map
	Evaporative reduction coefficient	β	-	0.94	Calibrated (ETca meas.; bare soil period)
VEGETATION	Maximal transpiration coefficient	Kcb_{max}	-	1.15	Literature (FAO-56 Allen et al., 1998)
	Exponent of the transpiration	E_{trp}	-	0.34	Calibrated (ETca meas.; non-stressed vegetation period)
	Transpiration reduction coefficient	Dft	-	0.45	Literature (FAO-56 Allen et al., 1998)
	Root growth rate	Vpr	m.°C	0.0015	Literature (STICS Brisson et al., 2003)
IRRIGATION	Irrigation depth	D_I	mm	30	Agricultural practices
	Number of days before harvest for irrigation ending	I_{end}	day of year	45	Agricultural practices

189 *Table 1: List of the 27 parameters of the crop model (i.e. 16 for the SAFY model, 9 for the water balance*

190 *model and 2 for the automatic irrigation module) with their initial value or range and the source of data.*

2.2. Study area

The study was carried out in the south west of France, near Toulouse (*Figure 1*). We focused on two departments (i.e. *division of the French territory according to administrative boundaries*): Haute-Garonne and Gers. The climate is temperate mild, with rainy springs and warm and dry summers (temperature often exceeding 35°C). The Haute-Garonne department is characterized by a wide plain stretching across the north and a mountainous region in the south that is a part of the Pyrenean range. The Gers department is characterized by hilly landscapes. Half of Haute-Garonne and up to 70% of Gers are covered by agricultural land. Haute-Garonne and Gers are respectively covered by about 20 000 ha and 48 000 ha of irrigated maize. In the study area, maize fields are sown from mid-April to early June, and harvest takes place from mid-August (mainly for silage maize) to late October.

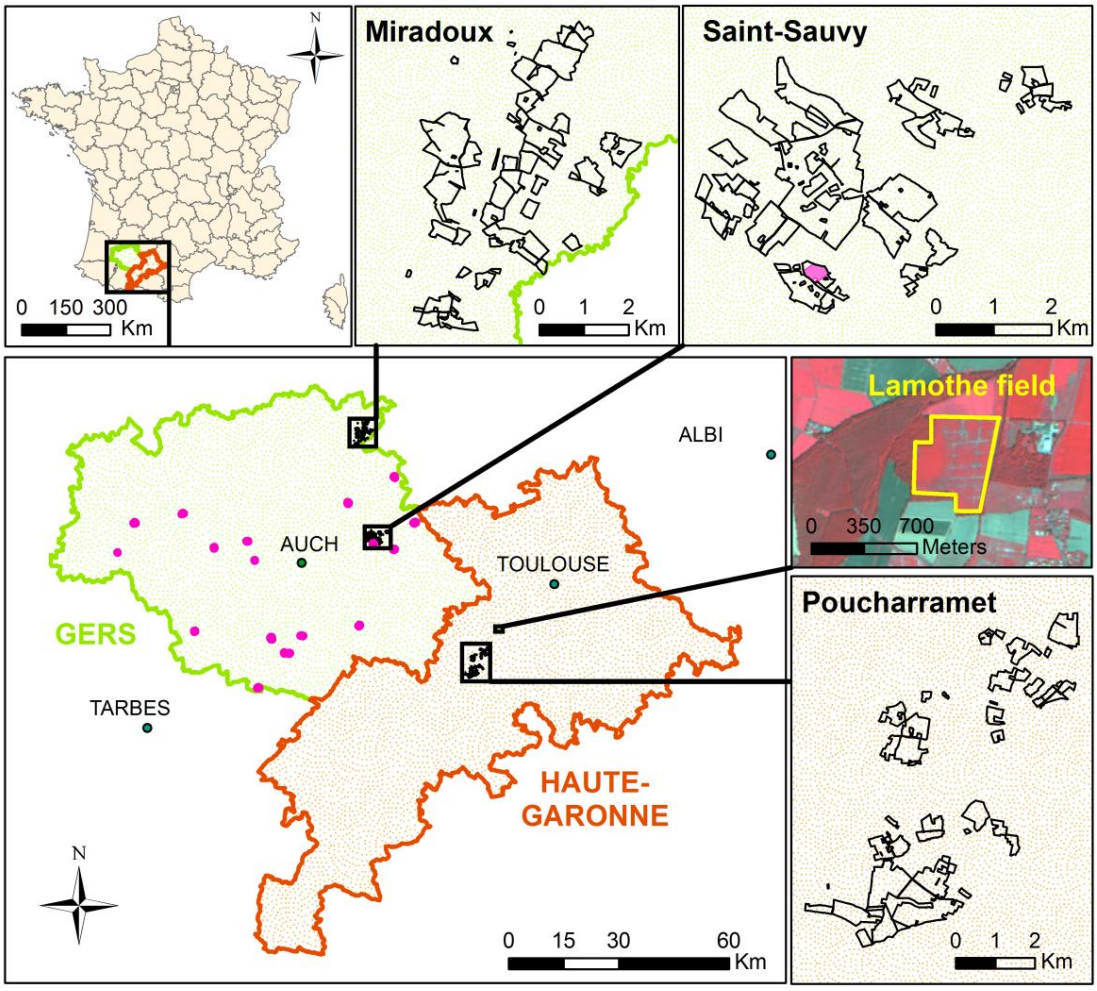

Figure 1: Location of the study area. Haute-Garonne and Gers departments are in orange and green, respectively. The "Lamothe" (LAM) experimental field is in yellow. Pink points represent the 18 maize fields and black region of interest represent the three irrigated zones (Miradoux, Saint-Sauvy and Poucharramet).

2.3. Dataset over the LAM field

2.3.1. Site description

The "Lamothe" experimental field (referred to as "LAM field") was instrumented in 2005 to monitor vegetation growth, soil water dynamics, turbulent energy, water and $C0_2$ fluxes. This 32.2 ha site is located close to a river in a large valley (*Figure 1*). It belongs to an experimental farm managed by the Purpan Engineering School and takes part of the European research infrastructure "Integrated Carbon Observation System" (ICOS, [https://icos-eco.fr/]) and of the "Regional Spatial Observatory" (OSR, [http://www.cesbio.ups-tlse.fr/fr/osr.html]). The LAM field is characterized by an irrigated silage maize/rainfed winter wheat rotation. We used four years of data over maize in 2006, 2008, 2010 and 2012, which correspond to years when maize was sown. The LAM field has a homogenous clay (around 50% clay, 36% loam and 14% sand) deep soil (around 1.5 m), presenting a large water storage capacity. We used a mean value of 0.36 $m^3.m^{-3}$ for the volumetric water content at field capacity (H_{fc}) and 0.17 $m^3.m^{-3}$ for the wilting point (H_{wp}). We did not evaluate the automatic irrigation module over this field as irrigation practices were not representative of those usually done in the south west of France. Actual irrigation data were forced in the model instead.

2.3.2. Flux data

Turbulent fluxes of water vapour (actual crop Evapotranspiration, *ETca*) are measured continuously according to the Eddy-Covariance method (Moncrieff et al., 1997; Baldocchi, 2003; Aubinet et al., 2012). The flux tower was installed in the middle of the field and the Eddy-Covariance system set-up was designed in order to catch the turbulent fluxes from a representative area (*footprint*) of the whole crop

plot. The height of the instruments (3.65 m) was chosen to be higher than crops at their maximum development and optimize the footprint area (Béziat et al., 2009). The Eddy-Covariance system combined a 3D sonic anemometer (CSAT3) with a high frequency infrared gas analyzer (LI-7500, 20 Hz). Flux calculation, filtering, quality controls and gap filling were performed following the CarboEurope-IP recommendations (Aubinet et al., 2012).

2.3.3. Meteorological data

The LAM field is equipped with a standard weather station. It provides measurements of air temperature, relative humidity, global and net radiations, wind speed and direction at 3.65 m height, precipitation and atmospheric pressure. The total precipitation during the four experimental maize seasons (*i.e. from date of emergence to harvest in 2006, 2008, 2010 and 2012*) was 118, 188, 173 and 125 mm, respectively. All flux and meteorological data were originally recorded and processed at half-hourly time step. The data were thus integrated or averaged to obtain daily time scale estimates allowing the comparison with the model outputs.

2.3.4. Biomass destructive measurements

Dry Aboveground Mass (*DAM*) data were collected from LAM field with a destructive method during four maize growing seasons between 2006 and 2012 at the rate of five times a year. Each time, twenty plants were harvested within the footprint, dried at 55°C, during at least 72h, and then weighed.

2.4. Validation datasets: the 18 fields and 3 irrigated zones

A validation set of 18 maize fields (0.5 ha to 24 ha) have been monitored by the water manager (CACG, i.e. Compagnie d'Aménagement des Coteaux de Gascogne) during the 2013 growing season. The CACG is in charge of irrigation recommendations to the farmers. All fields were located in the Gers department (*Figure 1*). The irrigation practices including dates and applied water depth (in mm) were recorded and provided by farmers. The total irrigation depth applied during the growing season (in mm) was calculated for each field and compared with the simulations (automatic irrigation module). Water is

applied to all these fields with sprinkler irrigation systems.

Three irrigated zones (Miradoux, Saint-Sauvy and Poucharramet) (*Figure 1*) also monitored by the CACG have been used for the validation of the total irrigation depth. They correspond to associations of farmers sharing a global irrigation plan (hereafter referred to as "ASA" for "Authorised Syndical Association"). Poucharramet ASA's irrigated water supplies have been studied since 2006. Miradoux and Saint-Sauvy ASA's irrigated water supplies were studied for 2013 and 2014 growing seasons. Poucharramet, Miradoux and Saint-Sauvy ASA are respectively covered by about 450 ha, 165 ha and 135 ha of irrigated grain maize. For these three ASA, applied irrigation water comes from surface resource (rivers recharged either by lakes, canals or mountains' reservoirs depending on location). The water is collected in the river with a pumping station and then conveyed throughout the fields using a pipe network. Sprinkler irrigation systems are used in the three ASA. Meteorological data over the area have been estimated by Météo-France using the mesoscale atmospheric analysis system SAFRAN (i.e. Système d'Analyse Fournissant des Renseignements Adaptés à la Nivologie ; Durand et al., 1993). This dataset includes air temperature at 2m above the ground (*Ta*), incoming global radiation (*Rg*), reference evapotranspiration (ET_0) and precipitation (*P*). ET_0 is derived from climatic parameters according to the Penman-Monteith equation recommended by FAO (Allen et al., 1998).

The data are available every 6h over a 8 km spatial resolution grid. Vidal et al. (2010) performed an evaluation of SAFRAN data all over the French territory and found an RMSE ≈ 40 W/m² for Rg and an RMSE ≈ 0.6 °C for Ta. Data used to force the model (daily mean Ta, daily mean Rg, daily ET_0 and cumulated daily P) were calculated for each field over the study area, by using the nearest grid point.

Soil characteristics of the fields (H_{fc}, H_{wp} and *SD; see Table 1*) have been extracted from a soil map covering the two departments. This map (1/ 250 000) results from the IGCS (i.e. Inventaire, Gestion et Conservation des Sols) program, provided by GisSol (i.e. Groupement d'intérêt scientifique Sol) group [https://www.gissol.fr/le-gis/programmes/inventaire-gestion-et-conservation-des-sols-igcs-67], and

reports the main structural units of the area. The database related to the map provides for each class the soil depth and the percentage of clay, silt and sand. Soil texture was found using the French "Aisne" soil texture triangle (Jamagne et al., 1977; Baize and Jabiol, 1995). The volumetric water contents at field capacity (H_{fc}) and at wilting point (H_{wp}) were retrieved through the use of a class pedotransfer function (Bruand et al., 2003). For the 18 maize fields, the soil depth (*SD*) extracted from the map was compared to those provided by farmers. The impact of *SD* on the simulated total irrigation depth is presented in the results section.

2.5. Remotely sensed GAI and FCOVER

The Green Area Index (*GAI* in $m^2.m^{-2}$) and green cover fraction (*FCOVER*) time series were estimated from several high spatial and temporal resolution optical images (*Figures 2 and 3*) using the BVNet tool (i.e. Biophysical Variables neural NETwork, Weiss and Baret, 1999; Weiss et al., 2002). BVNet enables the estimation of biophysical variables (GAI, FAPAR and FCOVER) from the inversion of the radiative transfer model PROSAIL (Baret et al., 1992) using artificial neural network. The BVNet tool uses the Green, Red and NIR spectral bands, and the SWIR band whenever available. It computes GAI taking into account the spectral and directional characteristics (illumination and viewing angles) of the remote sensing data.

Formosat-2 (8 m resolution, daily revisit) and SPOT (20 m, monthly revisit) data have been available since 2006 over the LAM field and Poucharramet ASA. In addition, other satellite datasets covering a larger area including the 18 fields, Miradoux ASA and Saint-Sauvy ASA have been available since 2013. We thus combined Landsat-8 (30 m, 16-day revisit), Deimos-1 (22 m, 3-day revisit) and the SPOT4-Take5 experiment (20 m, 5-day revisit) [http://www.cesbio.ups-tlse.fr/multitemp/] datasets. The combination of datasets permits to observe the whole maize growing seasons with a temporal resolution close to that provided by the Sentinel-2 data (A and B). The satellites have also been chosen for their high spatial resolution (30 m or less) which is an important criteria given the mean size of agricultural fields in the

study area (approximately 20 ha).

The remotely sensed GAI time series were used in the previous study (Battude et al., 2016) to calibrate the SAFY model in order to provide daily GAI and biomass production estimates. The GAI and FCOVER were interpolated with a double logistic function (see Battude et al., 2016) providing daily time series used as inputs in the water balance module.

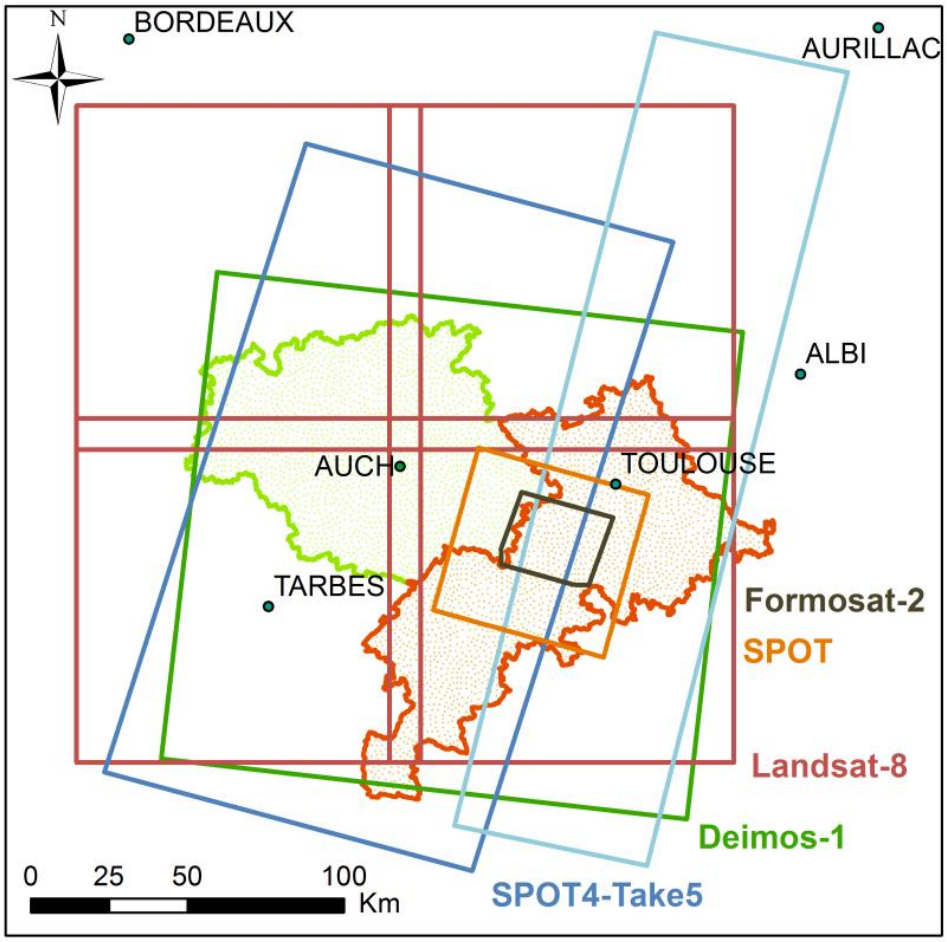

Figure 2: Location of the various image scenes (Formosat-2 in grey; SPOT in orange; SPOT4-Take5 in blue; Landsat-8 in red; Deimos-1 in green).

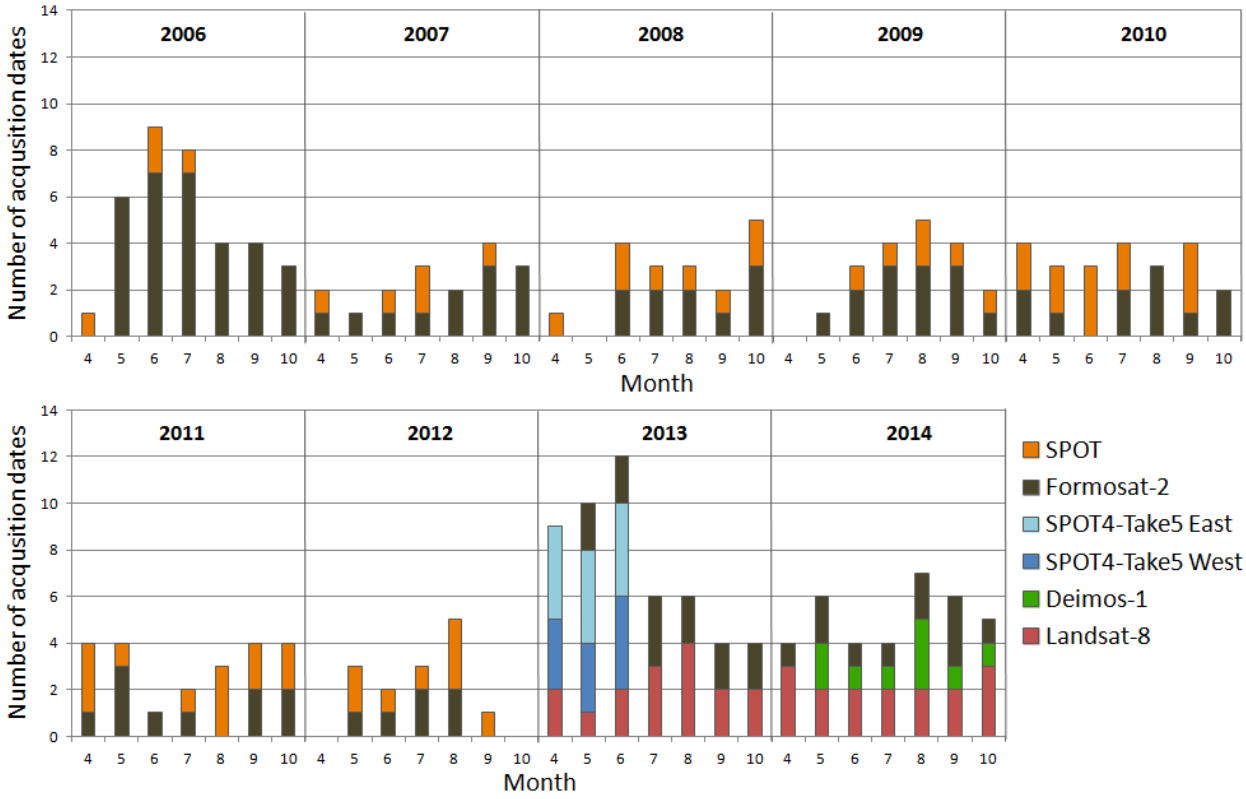

Figure 3: Schedule of images acquisitions for the different sensors. Only the maize growing periods (April to October) are displayed.

2.6. Calibration of model parameters

2.6.1. SAFY model parameters

We use the sixteen SAFY model parameters (*Table 1*) calibrated in the previous study (see Battude et al., 2016). Some parameters were fixed according to a literature review (ε_c, T_{min}, T_{opt}, T_{max}, β_0, K_{ext}, HI) and the remaining ones (D_0, PI_a, PI_b, RS, S_{TT}, SLA_0, LTC, $ELUE_p$ and PMI) were optimized using the remotely sensed GAI time series. This calibration leads to daily simulated GAI and biomass.

2.6.2. Water balance model parameters

The nine water balance model parameters (*Table 1*) include five soil parameters (SLT_1, SD, H_{fc}, H_{wp} and β) and four vegetation parameters (Kcb_{max}, E_{trp}, Dft and Vpr). Except for the surface layer thickness (SLT_1), the soil parameters needed for the definition of the storage capacity (H_{fc}, H_{wp} and SD) are field

specific. They vary spatially and depend on the soil type. Their values are determined with *in situ* measurements or information extracted from the soil map (see section 2.4). Kcb_{max} and *Dft* are fixed according to the FAO recommendations (Allen et al., 1998). The *Vpr* parameter is set according to the value used for maize crop in the STICS model (Brisson et al., 2003).

The remaining two parameters (β and E_{trp}) were calibrated using ETca measured by the Eddy-Covariance method. The calibration procedure was performed in two successive steps with a cost function based on the Root Mean Square Error (RMSE) computation (*Figure 4*). We firstly calibrated β over the bare soil period. Then, we calibrated E_{trp} over the non-stressed vegetation period (based on the calculation of the relative humidity (*RH*) of the two first soil layers). The calibration was done for each year. As the values of each parameter were quite similar whatever the year, we decided to use the four-year averaged value for each parameter. As simulation begins at 1st January, the soil water storage capacity is regarded as full at this date. Soil diffusive fluxes have not been taken into consideration.

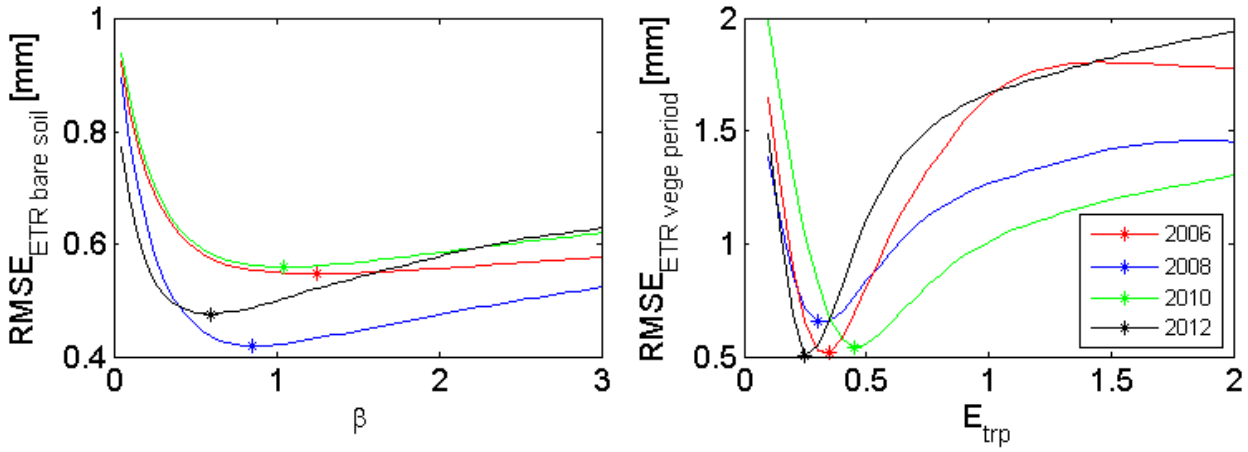

Figure 4: Calibration of β and E_{trp} parameters for the four studied years. The β parameter is calibrated on bare soil period measurements of ETca and the E_{trp} parameter is calibrated on non-stressed vegetation period ETca measurements.

2.6.3. Automatic irrigation module parameters

The irrigation parameters (D_I, I_{end}) values are set according to mean agricultural practices. When the

337 "automatic mode" is activated, a 30 mm irrigation depth (D_I) is applied at each irrigation event. 45-day
338 delay before harvest (I_{end}) is set for irrigation ending. If the irrigation depth exceeds the total soil water
339 storage capacity, the excess water is removed from the original 30 mm amount and a lower irrigation
340 depth is simulated by the model.

341 2.7. Model evaluation

342 A four-year dataset of ETca was used to calibrate the model (i.e. calibration of β and E_{trp}
343 parameters) and DAM destructive measurements were used for the validation. The 18 maize fields and
344 three irrigated zones (ASA) were used to evaluate the automatic irrigation module, comparing the water
345 supplies provided by the farmers with those simulated by the model. For the three ASA, the model was
346 run over all maize fields located into the irrigated zone; irrigation depths were cumulated and the total
347 depth for the growing season was thus compared to the data given by the water manager.

348 In this study, we compared ETca and total irrigation depths simulated using the standard crop
349 coefficient method and those obtained using the remotely sensed Kcb (i.e. the Kcb estimated from the
350 daily GAI simulated by SAFY, optimized using the remotely sensed GAI). We also used a soil map that
351 provides the soil depth and the soil water content limits (field capacity and wilting point). Root depth is
352 closely linked to soil depth and depth of water infiltration. This value affects the amount of water
353 available and the number of irrigation events needed to reach the crop needs. Thus we evaluated the
354 impact of the use of soil properties estimated from the soil map on ETca estimates and on total
355 irrigation depths, comparing to results obtained using *in situ* estimates of the SC.

356 The model was run using the interpolated GAI estimated for each sampled area (i.e. *LAM field, 18*
357 *fields or ASA*) using the methodology presented in the previous study (Battude et al., 2016). The model
358 evaluation was performed using several statistical criterions including correlation coefficient (*R*), bias,
359 Root Mean Square Error (*RMSE*) and Relative Root Mean Square Error (*RRMSE*), calculated by dividing
360 the RMSE by the mean of the observed data.

3. RESULTS AND DISCUSSION

3.1. Results over the LAM field : Evapotranspiration and Biomass

The dynamics of daily simulated GAI and DAM over the four maize growing seasons were respectively compared to remotely sensed GAI and *in situ* measurements of DAM performed over the LAM field. Results are presented in *Figure 5*. In this section, the model was run with the forced mode (i.e. *using the total water supplies: rainfall and real irrigation*). Results show an overall good adequacy of the GAI and DAM from the emergence date to the harvest for the four years. The DAM dynamics of the four years is correctly reproduced by the model (R = 0.97; RRMSE = 23%).

ETca measurements performed over the LAM field during the four years according to the Eddy-Covariance method have been used for the calibration of two model parameters (β and E_{trp}). The daily simulated ETca was compared to these measurements. Results (*Figure 6*) show that the dynamics of ETca correlates well with measured values. The correlation analysis (*Figure 7a*) shows a good linear relationship between measured and estimated values of ETca during the growing period (R = 0.88; RRMSE = 20%). We observe an overall underestimation of ETca before plant emergence and after harvest. These two periods correspond to bare soil in the model. However, if the model considers a total absence of vegetation, it may be actually different. Indeed, we found a delay between the actual emergence date and that observed by the remote sensors. Furthermore, some crop residues still cover the soil after harvest and they are not simulated by the model. This can explain the observed underestimation of simulated ETca. However, the main goal is to accurately reproduce the ETca during the growing period in order to have good estimates of the plant water needs. Focusing on the growing season, some discrepancies are observed, such as at the beginnings of the years 2008 and 2010, when the model underestimates the ETca. In both cases, it happens when FCOVER is lower than 0.5 and when no significant water supply (neither rain nor irrigation event) occurs for a long time (up to 1 month).

During these periods, the simulated soil evaporation is underestimated. The activation of the diffusive fluxes [Eq. 11 with *Edif* = 1 and *Kdif* = 3.5] helped to reduce the water scarcity in the top and intermediate soil layers and to increase ETca during these periods (see *Figure 6*). However, as the ratio between evaporation and transpiration decreases while the vegetation grows, the activation of diffusive fluxes did not change significantly the ETca estimates for the whole growing season. Given that the activation of diffusive fluxes would imply the calibration of two more parameters and that it did not bring significant improvement of the cumulative ETca values, we chose not to activate it for the following work.

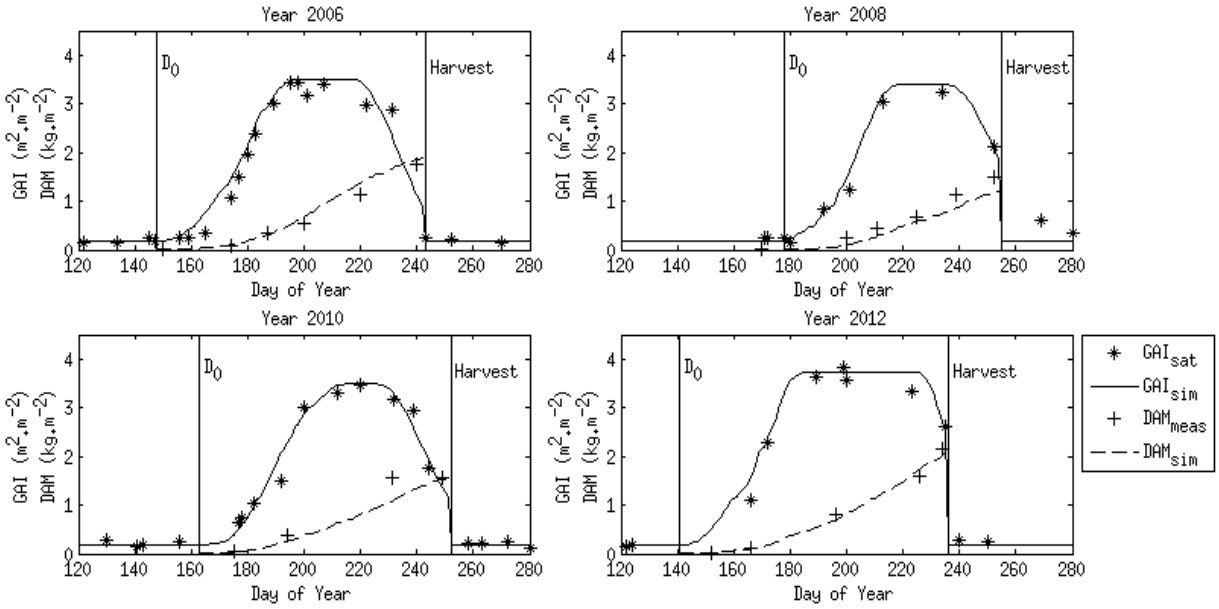

Figure 5: Dry Aboveground Mass (DAM) and Green Area Index (GAI) dynamics for the four maize growing seasons over the LAM field using the forced mode. Simulated GAI is compared to remotely sensed GAI (used for the model calibration) and simulated DAM is compared to in situ measurements.

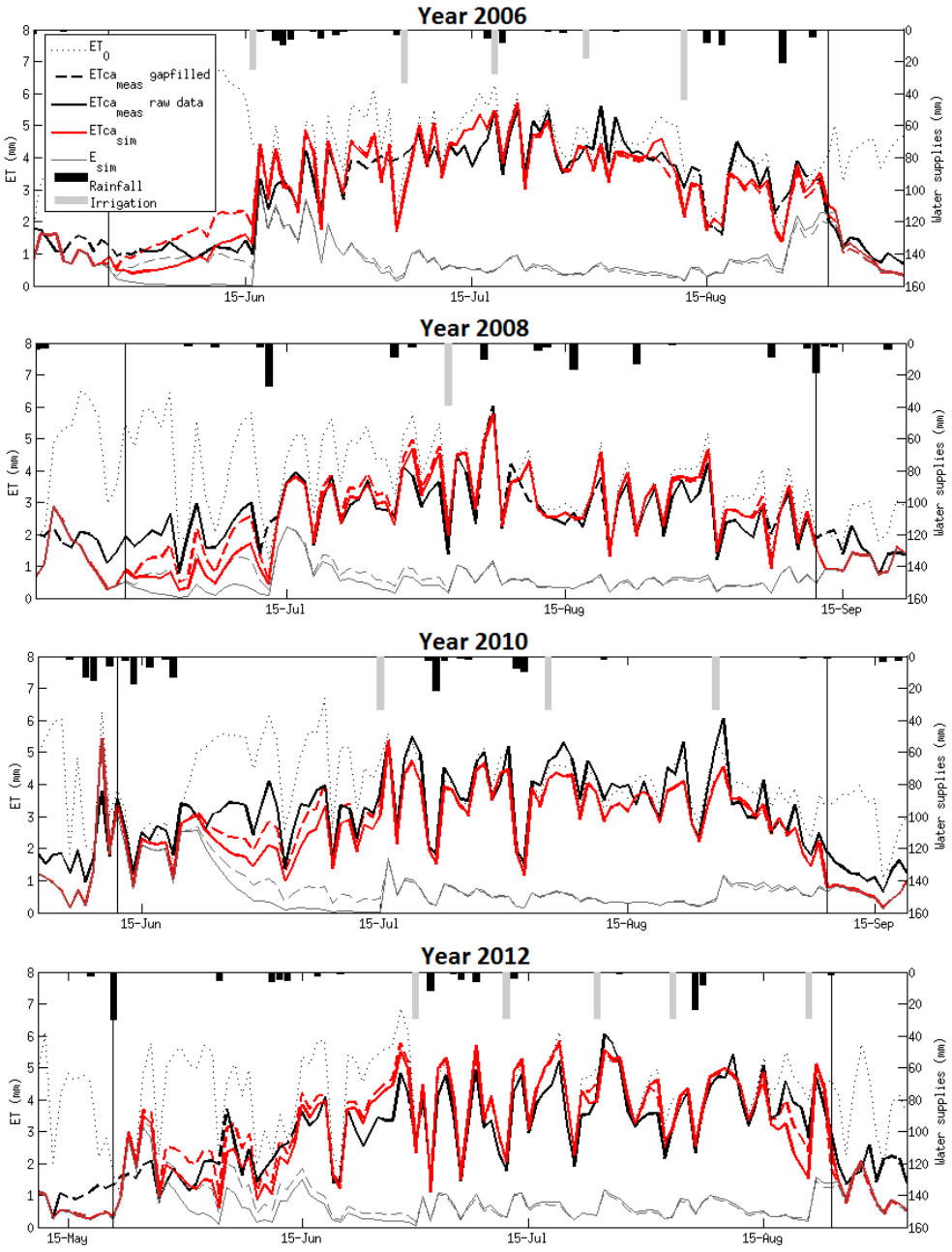

Figure 6: Comparison of measured (black line) and simulated (red line) actual crop Evapotranspiration (ETca) dynamics for the four maize growing seasons over the LAM field using the forced mode Dotted line represents reference evapotranspiration (ET_0). Grey line is the simulated evaporation (E). Dashed red and grey lines represent the simulated ETca and E when activating the diffusive fluxes. The two vertical black lines correspond to the simulated emergence date and to the actual harvest date, respectively. ETca measurements have been used for the calibration of two model parameters (β and Etrp).

3.2. Effect of the use of the soil map and standard Kcb values on ETca estimates over the LAM field

Since measurements of soil characteristics (H_{fc}, H_{wp} and SD) are rarely available over large areas, we used a 1/250 000 soil map that was available over the whole study area. Its coarse resolution implies that the soil characteristics estimated from the map differ from local conditions. To evaluate the potential effects of this difference on ETca estimates, we ran the model over the LAM field using the soil characteristics provided by both the soil map and *in situ* data. The soil water storage capacity (SC) is equal to 285 mm using *in situ* measurements and 172.5 mm using the soil map. This difference led to a slight decrease and larger dispersion of ETca estimates when using the soil map (*Figure 7b*) compared to the use of local soil measurements (*Figures 7a*).

To estimate crop water needs, the CACG uses standard Kcb (i.e. basal crop coefficient) values based on the knowledge of the phenological stages of the crop under standard conditions (i.e. tables proposed by Arvalis - Institut du Végétal). This method presents two major limitations: the phenological stages are not accessible over large areas and "standard conditions" do not mean "actual conditions". As an alternative, we propose to estimate the Kcb from the daily GAI simulated by SAFY [Eq. 10] optimized using the remotely sensed (RS) GAI. The use of remotely sensed Kcb, hereafter referred to as "*RS Kcb*", permits to access differences that might occur between fields as demonstrated by several studies (Bausch et al., 1987; Neale et al., 1989; Hunsaker et al., 2003; Glenn et al., 2011). We compared ETca estimates over the LAM field using both methods. Results (*Figures 7a and 7c*) show that the use of the standard Kcb leads to poorer ETca estimates (R = 0.77 instead of 0.88; RRMSE = 28% instead of 20%).

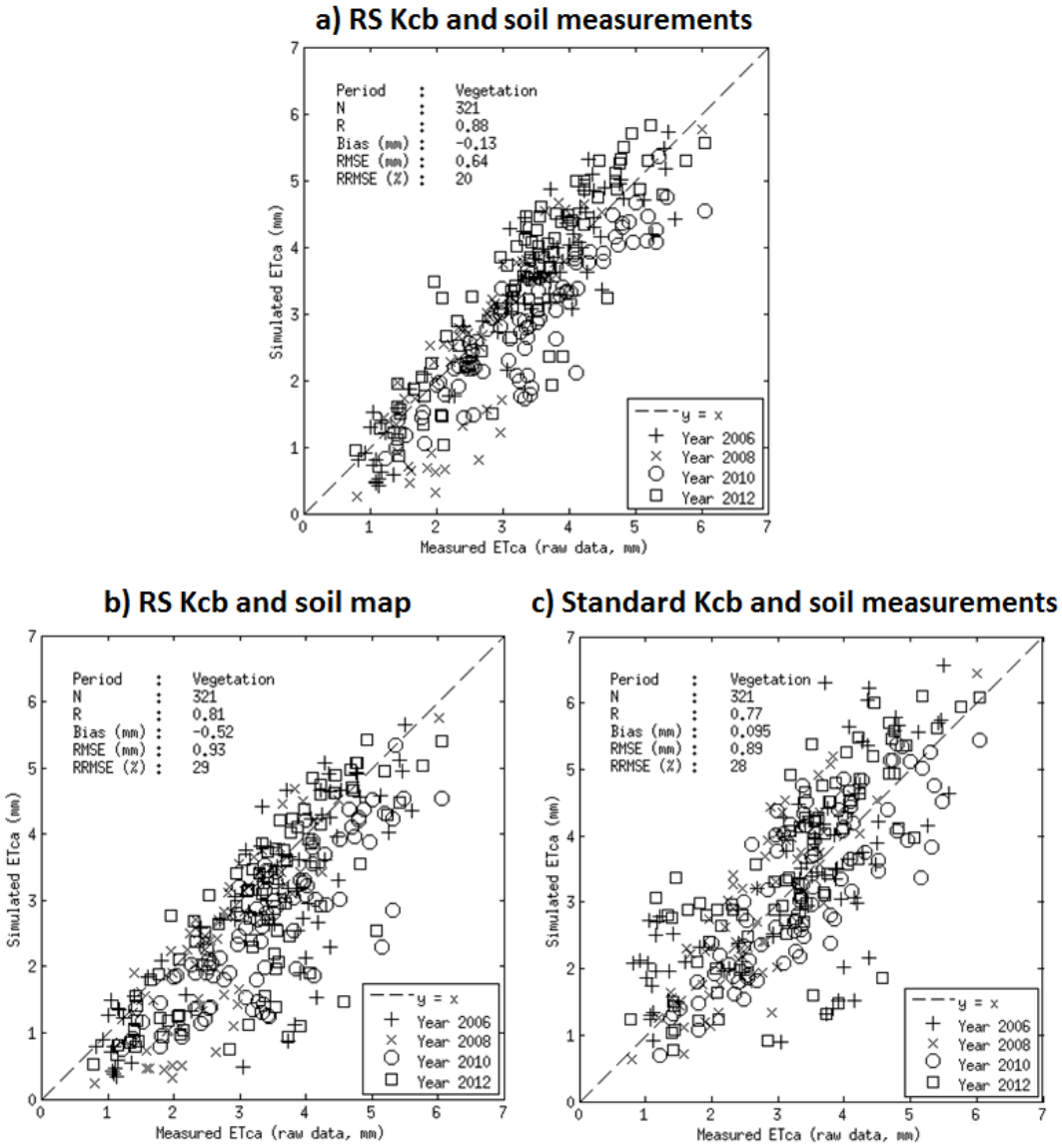

Figure 7: Comparison of measured and simulated daily ETca [mm] of maize for the four growing seasons (vegetation period) over the LAM field with the forced mode, when using a) the in situ soil depth and the remotely sensed (RS) Kcb, b) the map soil depth and the RS Kcb and c) the in situ soil depth and the standard Kcb.

3.3. Validation over 18 maize fields : total irrigation depth

The model was run by activating the automatic irrigation module over a set of 18 maize fields to evaluate its ability to trigger irrigations events according to the water stress level assessment. We used

the RS Kcb and the maximal soil depth (*SD*). SD was initialized using values provided by farmers. H_{fc} and H_{wp} parameters were extracted from the soil map.

Figure 8a shows the comparison between the total irrigation depths provided by farmers during the growing season and those recommended by the model. Overall, despite an observed bias of 20 mm, the activation of the automatic mode resulted in a good reproduction of the farmers' practices in terms of total water amount (R = 0.79; RRMSE = 18.8%). The negative bias can be explained by the fact that the model triggers irrigation when crop water stress occurs, while farmers are more careful and tend to irrigate before water stress occurs. In addition, farmers follow the advice of the water manager who calculates the crop water requirement using the standard Kcb and this method can potentially overestimate the water need.

3.3.1. Effect of the use of the soil map on the total irrigation depth

We then evaluated the impact of the use of the soil map on the simulated total irrigation depth over the 18 fields using the soil depth (*SD*) provided by the soil map and that provided by farmers. *Figure 8b* shows an overall decrease of the amount of total irrigation depths when using the soil map compared to the use of local farmer-provided soil depth values (*Figure 8a*) (bias of -55 mm instead of -20 mm). This occurs because the value of soil water storage capacity (*SC*) [Eq. 5] was larger using soil map: 150 mm on average vs. 80 mm using farmers' data. As the SC is almost full at the plant emergence (only the first layer can be incomplete since evaporation occurs), the use of a higher value for SC leads to less water supplies.

3.3.2. Effect of the use of the standard Kcb values on the total irrigation depth

Finally, we looked at the total irrigation water supplies simulated over the 18 maize fields using the standard Kcb values. *Figure 8c* shows that the use of the standard Kcb values led to a larger dispersion of the total irrigation depths compared to those obtained with RS Kcb (*Figure 8a*) (R = 0.68 with standard Kcb instead of R = 0.79 with RS Kcb). *Figure 9* shows the comparison of standard and RS Kcb time series

for the 18 maize fields: the RS Kcb evolves in the same way as the simulated GAI, whereas the standard Kcb evolves gradually according to the phenological stages. Furthermore, we can see for some fields that the standard Kcb value is higher than the RS Kcb at the beginning of the growing season. This can lead to a higher estimation of crop water needs and thus increase the number of simulated irrigation events. *Figure 10* shows the effect of the different Kcb estimates: standard Kcb values higher than RS Kcb (near day 200 and day 220) led to an increase of simulated water needs followed by two additional irrigations.

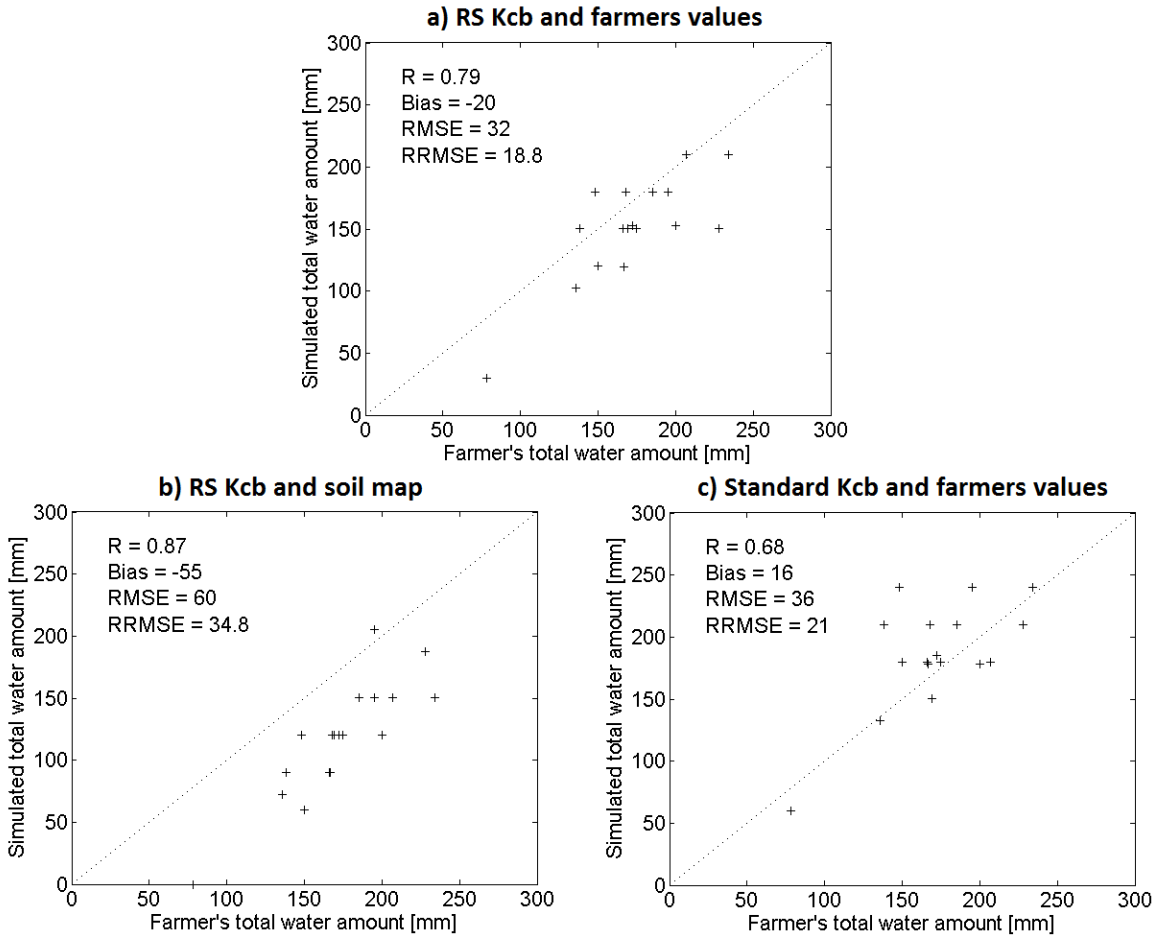

Figure 8: Comparison of total irrigation depth [mm] applied by farmers over 18 maize fields and the recommended irrigation of the combined SAFY-FAO model. For modeling we used a) in situ soil depth provided by farmers and RS Kcb, b) soil depth provided by the soil map and RS Kcb and c) in situ soil depth provided by farmers and standard Kcb.

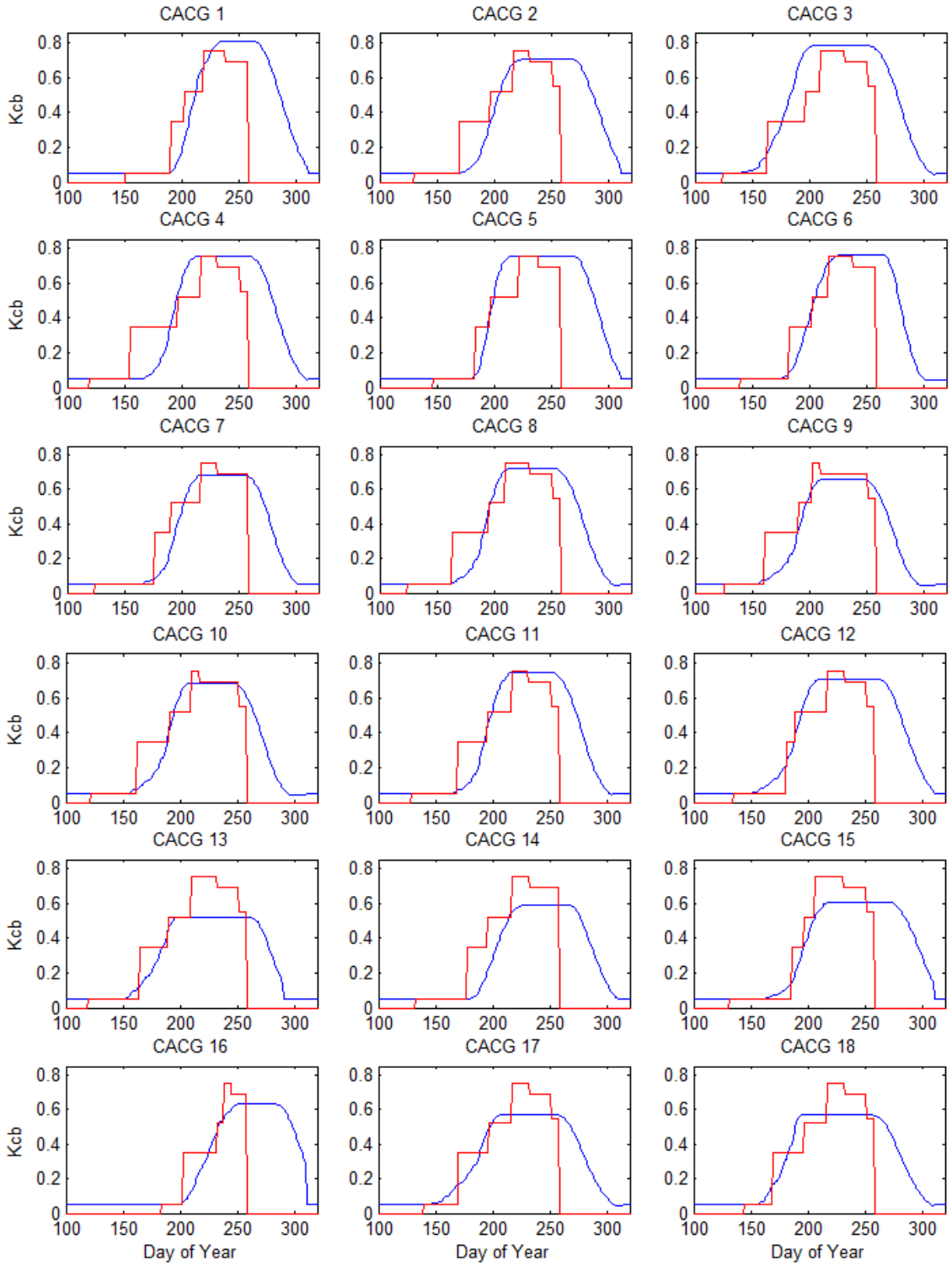

Figure 9: Comparison of standard Kcb (in red) and remotely sensed Kcb (in blue) for the 18 maize fields in year 2013. Standard Kcb ends in the middle of September, when the irrigation period ends (several weeks before harvest).

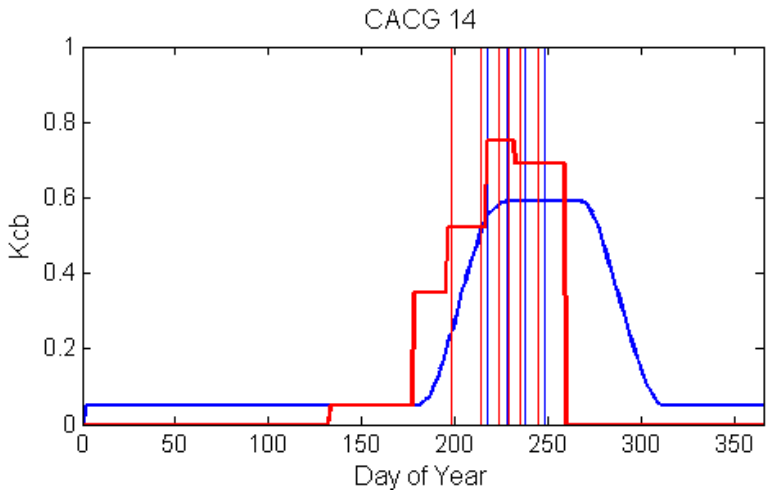

Figure 10: Comparison of standard Kcb (in red) and remotely sensed Kcb (in blue) for a maize field in year 2013. Vertical red and blue lines represent the irrigation events simulated for the two cases (6 irrigation events in case of standard Kcb and 4 irrigation events when using the RS Kcb). Standard Kcb ends in the middle of September, when the irrigation period ends (several weeks before harvest).

3.4. Validation over 3 irrigated zones: total irrigation depth

We ran the model over three irrigated zones (ASA) and compared the total irrigation depth simulated (in mm) to the actual total irrigation depth (in mm). Water managers estimate there is an average water loss of 12% due either to leaks during the transport of the water in the pipes (around 1-2%) or to the sprinkler irrigation system (around 3-10%). We thus removed 12% from the recorded annual irrigation depths.

In this section, we ran the model with the soil data provided by the soil map. For Miradoux and Saint-Sauvy ASA, the soil water storage capacity (*SC*) extracted from the soil map varies from 24 mm to 195 mm (*Figure 11*). For all the fields of the ASA of Poucharramet, the map provides a SC value higher than 170 mm. A high underestimation of the irrigation water amount by the model is observed in this ASA (*Figure 12a*). Simulated total irrigation depths for the two other irrigated zones (Miradoux and Saint-Sauvy) are closer to the observed depths. Given the results obtained over the 18 maize fields in the previous section and the impact of the SC, we chose to limit the soil depth and thus the root depth

[Eq. 6] at a maximum value of 80 cm considered as more likely by farmers. For the ASA of Miradoux and Saint-Sauvy, many of the fields are located on shallow soils (<80 cm) with low SC. For this reason, the limitation of the soil depth (*SD*) had a lower impact on the estimated total irrigation depth. For the ASA of Poucharramet, the modeled total irrigation depths are still lower than the observed values, but the mean bias is a bit reduced using lower SC (-93 mm instead of -108 mm; *Figure 12b*). Part of the negative bias may be explained by the SC that may remain too high for some fields despite the applied reduction. The underestimation may also be partly due to over-irrigation practices carried out by farmers, linked with an overestimation of water needs by water managers that use the standard Kcb. Despite this bias, the model reproduces correctly the inter-annual variability observed across years and ASA (R = 0.8).

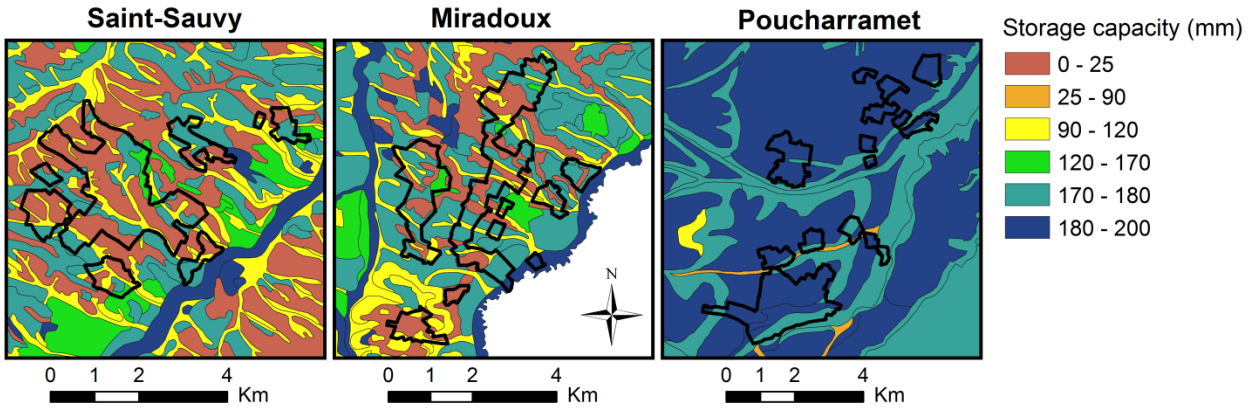

Figure 11: Soil water storage capacity of the three ASA (black polygons) extracted from the soil map.

a) *b)*

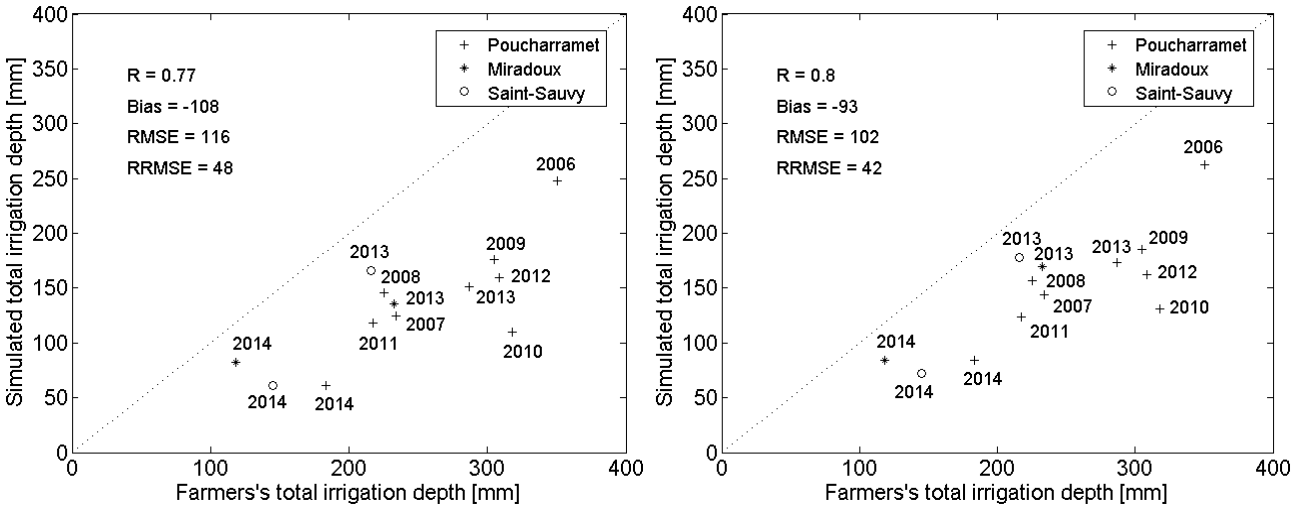

Figure 12: Comparison of total irrigation depth [mm] applied by farmers and the recommended irrigation of the combined SAFY-FAO model over irrigated maize fields of the three ASA for different years using a) the soil depth provided by the soil map b) a maximum soil depth of 80 cm.

4. CONCLUSION

One main objective of this study was to evaluate the potential of the SAFY-FAO model combined with remote sensing optical imagery to provide reliable estimations of water needs and total irrigation depths of irrigated maize crop over large areas. For that purpose, we used a new version of the SAFY model proposed by Battude et al. (2016) coupled with a water balance module adapted from FAO-56 method (Allen et al., 1998). The SAFY-FAO model was chosen for its suitablility for spatial approaches through the use of remotely sensed GAI time series. Another objective was to evaluate the impact of different methods used to determine the soil water storage capacity (SC) and the basal crop coefficient (Kcb) on simulated ETca and total irrigation depths.

After calibration over the experimental field using a four-year *in situ* ETca dataset, the model outputs were evaluated over 18 maize fields and three irrigated zones (ASA) for which the total irrigation depth applied during the growing season were known. Overall, good results were obtained for biomass production (R = 0.97; RRMSE = 23%) and ETca estimates (R = 0.88; RRMSE = 20%) after calibration over the experimental field. The model also reproduced well the total irrigation depths over the 18 maize fields (R = 0.79; RRMSE = 18.8%). We observed an underestimation of the total irrigation depth (-93 mm) for the three ASA. This might be explained by either the use of the standard Kcb by water managers (leading to an overestimation of water needs), over-irrigation practices or even the SC values that might be too high when using the soil map. Despite this, the model reproduces correctly the trends observed between years and ASA (R = 0.8).

This work permitted to highlight the impact of different methods to estimate the SC and the Kcb on ETca and on the total irrigation depth over large areas. The use of a standard Kcb led to a larger

526 dispersion on ETca compared to results found using a remotely sensed (RS) Kcb (R = 0.77 with standard
527 Kcb and R = 0.88 with RS Kcb). Same conclusions were drawn for the total irrigation depth over the 18
528 maize fields (R = 0.68 with standard Kcb and R = 0.79-0.87 with RS Kcb). Furthermore, the standard Kcb
529 requires the knowledge of the phenological stages of the crop that are not available over large areas and
530 even difficult to accurately obtain at field scale. Such results highlight the potential of the RS Kcb to
531 improve irrigation water management.

532 The impact of various SC estimations (soil map vs *in situ* measurements or farmers' values) on ETca
533 and total irrigation depths was also investigated. Results highlighted that the soil depth (SD) provided by
534 the soil map induced negative bias on simulated ETca and total irrigation depth because of a high
535 imprecision on soil properties (SD, H_{fc} and H_{wp}) partly due to its coarse spatial resolution. Future work
536 will investigate ways to retrieve SD, for example using the future Global Soil Map given at 90 m spatial
537 resolution ([http://www.globalsoilmap.net/]).

538 This work also points out some limitations that should be investigated in future work. We chose to
539 calibrate the water module using four-year averaged parameters based on ETca measurements. The
540 validation using ETca measurements over other fields or years may allow evaluating the robustness of
541 the calibrated parameters and the associated error.

542 We also chose to disable the diffusive fluxes in soils as results showed minor improvement on
543 simulated ETca during the whole growing season. However, this process should be taken into account
544 when simulating annual soil water budget.

545 The model was used on irrigated crops with a diagnostic approach. In the future, we planned to
546 investigate its prognostic potential and enlarge its application on rainfed crops. This study demonstrates
547 the high potential of an agro-meteorological crop model combined with high spatial and temporal
548 resolution remote sensing data for a large-scale monitoring of total irrigation depths over maize fields. It
549 offers encouraging perspectives when using Sentinel-2 images in the near future. The Sentinel-2 dataset,

550 available since May 2015, covering the whole globe and freely available, will be really interesting for
551 future applications over large areas.

552 # ACKNOWLEDGMENTS

553 This work is part of the MAISEO project (four-year FUI program, 2012-2016 financed by FEDER and
554 BPI France). Observation data were collected at the Regional Spatial Observatory (OSR). OSR facilities
555 and staff are funded and supported by the Observatory Midi-Pyrenean, the University Paul Sabatier of
556 Toulouse (UPS) and CNRS (Centre National de la Recherche Scientifique), CNES (Centre National
557 d'Etudes Spatiales), IRD (Institut de Recherche pour le Développement). We are grateful to the team of
558 the Lamothe experimental farm for facilitating access to their field. Thanks to Météo France and
559 specially François Besson and Sébastien Prats for the supply of SAFRAN meteorological data covering the
560 study area. We are also grateful to the members of the IGCS program and ENSAT (particularly Maritxu
561 Guiresse) providing the soil map and Laurent Rigou (A.S.U.P.) for his support. Thank to Richard Escadafal
562 for proofreading the paper. Special thank to the CESBIO team (Claire Marais Sicre, Bartosz Zawilski,
563 Nicole Ferroni and Jean-François Dejoux) and CACG team (Mathieu Lasserre, Nicolas Laborde and Céline
564 Joandet-Péraut) and all the persons who participated in the collection of data.

565 # REFERENCES

566 Allen, R.G., Pereira, L.S., Raes, D., Smith, M., 1998. Crop evapotranspiration-Guidelines for computing
567 crop water requirements-FAO Irrigation and drainage paper 56. FAO, Rome 333 pp.
568 Amos, B., Walters, D. T., 2006. Maize Root Biomass and Net Rhizodeposited Carbon. Soil Science Society
569 of America Journal 70(5), 1489–1503. doi:10.2136/sssaj2005.0216
570 Aubinet, M., Vesala, T., Papale, D., 2012. Eddy Covariance: A practical guide to measurement and data
571 analysis. Springer Atmospheric Sciences.
572 Baize, D., Jabiol, B., 1995. Guide pour la description des sols. INRA, éditions Quae.

573 Baldocchi, D.D., 2003. Assessing the eddy covariance technique for evaluating carbon dioxide exchange
574 rates of ecosystems: past, present and future. Global Change Biology 9, 479–492. doi:10.1046/j.1365-
575 2486.2003.00629.x
576 Baret, F., de Solan, B., Lopez-Lozano, R., Ma, K., Weiss, M., 2010. GAI estimates of row crops from
577 downward looking digital photos taken perpendicular to rows at 57.5° zenith angle: Theoretical
578 considerations based on 3D architecture models and application to wheat crops. Agricultural and
579 Forest Meteorology 150, 1393–1401. doi:10.1016/j.agrformet.2010.04.011
580 Baret, F., Jacquemoud, S., Guyot, G., & Leprieur, C., 1992. Modeled analysis of the biophysical nature of
581 spectral shifts and comparison with information content of broad bands. Remote Sensing of
582 Environment 41(2-3), 133-142. doi:10.1016/0034-4257(92)90073-S
583 Baroni, G., Facchi, A., Gandolfi, C., Ortuani, B., Horeschi, D., van Dam, J.C., 2010. Uncertainty in the
584 determination of soil hydraulic parameters and its influence on the performance of two hydrological
585 models of different complexity. Hydrology and Earth System Sciences 14(2), 251-270.
586 doi:10.5194/hess-14-251-2010
587 Battude, M., Al Bitar, A., Morin, D., Cros, J., Huc, M., Marais Sicre, C., Le Dantec, V., Demarez, V., 2016.
588 Estimating maize biomass and yield over large areas using high spatial and temporal resolution
589 Sentinel-2 like remote sensing data. Remote Sensing of Environment 184, 668-681.
590 doi:10.1016/j.rse.2016.07.030
591 Bausch, W.C., Neale, C.M.U., 1987. Crop coefficients derived from reflected canopy radiation: a concept.
592 Transactions of ASAE 30(3), 703-709. doi : 10.13031/2013.30463
593 Béziat, P., Ceschia, E., Dedieu, G., 2009. Carbon balance of a three crop succession over two cropland
594 sites in South West France. Agricultural and Forest Meteorology 149, 1628–1645.
595 doi:10.1016/j.agrformet.2009.05.004
596 Brisson, N., Gary, C., Justes, E., Roche, R., Mary, B., Ripoche, D., Zimmer, D., Sierra, J., Bertuzzi, P.,

597 Burger, P., Bussière, F., Cabidoche, Y.M., Cellier, P., Debaeke, P., Gaudillère, J.P., Hénault, C., Maraux,
598 F., Seguin, B., Sinoquet, H., 2003. An overview of the crop model stics. European Journal of Agronomy
599 18, 309–332. doi:10.1016/S1161-0301(02)00110-7
600 Bruand, A., Fernández, P.P., Duval, O., 2003. Use of class pedotransfer functions based on texture and
601 bulk density of clods to generate water retention curves. Soil Use and Management 19, 232–242.
602 doi:10.1111/j.1475-2743.2003.tb00309.x
603 Cavero, J., Farré, I., Debaeke, P., Faci, J.M., 2000. Simulation of maize yield under water stress with the
604 EPICphase and CROPWAT models. Agronomy Journal 92, 679–690. doi:10.2134/agronj2000.924679x
605 Claverie, M., Demarez, V., Duchemin, B., Hagolle, O., Ducrot, D., Marais Sicre, C., Dejoux, J.-F., Huc, M.,
606 Keravec, P., Béziat, P., Fieuzal, R., Ceschia, E., Dedieu, G., 2012. Maize and sunflower biomass
607 estimation in southwest France using high spatial and temporal resolution remote sensing data.
608 Remote Sensing of Environment 124, 844–857. doi:10.1016/j.rse.2012.04.005
609 Constantin, J., Willaume, M., Murgue, C., Lacroix, B., Therond, O., 2015. The soil-crop models STICS and
610 AqYield predict yield and soil water content for irrigated crops equally well with limited data.
611 Agricultural and Forest Meteorology 206, 55–68. doi:10.1016/j.agrformet.2015.02.011
612 Dorigo, W.A., Zurita-Milla, R., de Wit, A.J.W., Brazile, J., Singh, R., Schaepman, M.E., 2007. A review on
613 reflective remote sensing and data assimilation techniques for enhanced agroecosystem modeling.
614 International Journal of Applied Earth Observation and Geoinformation 9, 165–193.
615 doi:10.1016/j.jag.2006.05.003
616 Droogers, P., Immerzeel, W.W., Lorite, I.J., 2010. Estimating actual irrigation application by remotely
617 sensed evapotranspiration observations. Agricultural Water Management 97, 1351–1359.
618 doi:10.1016/j.agwat.2010.03.017
619 Drouet, J.-L., Pagès, L., 2003. GRAAL: a model of GRowth, Architecture and carbon ALlocation during the
620 vegetative phase of the whole maize plant: Model description and parameterisation. Ecological

621 Modelling 165, 147–173. doi:10.1016/S0304-3800(03)00072-3
622 Duchemin, B., Fieuzal, R., Rivera, M.A., Ezzahar, J., Jarlan, L., Rodriguez, J.C., Hagolle, O., Watts, C., 2015.
623 Impact of sowing date on yield and water use efficiency of wheat analyzed through spatial modeling
624 and Formosat-2 images. Remote Sensing 7, 5951–5979. doi:10.3390/rs70505951
625 Duchemin, B., Maisongrande, P., Boulet, G., Benhadj, I., 2008. A simple algorithm for yield estimates:
626 Evaluation for semi-arid irrigated winter wheat monitored with green leaf area index. Environmental
627 Modelling & Software 23, 876–892. doi:10.1016/j.envsoft.2007.10.003
628 Duchemin, B., Hadria, R., Erraki, S., Boulet, G., Maisongrande, P., Chehbouni, A., Escadafal, R.G., Ezzahar,
629 J., Hoedjes, J.C.B., Kharrou, M.H., Khabba, S., Mougenot, B., Olioso, A., Rodriguez, J.-C., Simonneaux,
630 V., 2006. Monitoring wheat phenology and irrigation in Central Morocco: On the use of relationships
631 between evapotranspiration, crops coefficients, leaf area index and remotely-sensed vegetation
632 indices. Agricultural Water Management 79, 1–27. doi:10.1016/j.agwat.2005.02.013
633 Durand, Y., Brun, E., Mérindol, L., Guyomarc'h, G., Lesaffre, B., Martin, E., 1993. A meteorological
634 estimation of relevant parameters for snow models. Annals of Glaciology 18, 65–71.
635 Glenn, E.P., Neale, C.M.U., Hunsaker, D.J., Nagler, P.L., 2011. Vegetation index-based crop coefficients to
636 estimate evapotranspiration by remote sensing in agricultural and natural ecosystems. Hydrological
637 Processes 25(26), 4050-4062. doi:10.1002/hyp.8392
638 Hunsaker, D.J., Pinter, P.J., Barnes, E.M., Kimball, B.A., 2003. Estimating cotton evapotranspiration crop
639 coefficients with a multispectral vegetation index. Irrigation science 22, 95-104. doi:10.1007/s00271-
640 003-0074-6
641 Jamagne, M., Betremieux, R., Begon, J.C., Mori, A., 1977. Quelques données sur la variabilité dans le
642 milieu naturel de la réserve en eau des sols. Bulletin Technique d'Information 324–325, 627–641.
643 Jones, J.W., Hoogenboom, G., Porter, C.H., Boote, K.J., Batchelor, W.D., Hunt, L.A., Wilkens, P.W., Singh,
644 U., Gijsman, A.J., Ritchie, J.T., 2003. The DSSAT cropping system model. European journal of

agronomy 18, 235–265.

Kijne, J.W., Barker, R., Molden, D.J., 2003. Water Productivity in Agriculture: Limits and Opportunities for Improvement. CABI.

Lawless, C., Semenov, M.A., Jamieson, P.D., 2008. Quantifying the effect of uncertainty in soil moisture characteristics on plant growth using a crop simulation model. Field Crops Research 106(2), 138-147. doi:10.1016/j.fcr.2007.11.004

Maas, S.J., 1992. GRAMI: a crop growth model that can use remotely sensed information. ARS-91 USDA, Washington, DC.

Mailhol, J.C., Olufayo, A.A., Ruelle, P., 1997. Sorghum and sunflower evapotranspiration and yield from simulated leaf area index. Agricultural Water Management 35, 167–182. doi:10.1016/S0378-3774(97)00029-2

Moncrieff, J.B., Massheder, J.M., de Bruin, H., Elbers, J., Friborg, T., Heusinkveld, B., Kabat, P., Scott, S., Soegaard, H., Verhoef, A., 1997. A system to measure surface fluxes of momentum, sensible heat, water vapour and carbon dioxide. Journal of Hydrology 188, 589–611. doi:10.1016/S0022-1694(96)03194-0

Monteith J.L., 1972. Solar Radiation and Productivity in Tropical Ecosystems. The Journal of Applied Ecology 9(3), 747–766. doi:10.2307/2401901

Nana, E., Corbari, C., Bocchiola, D., 2014. A model for crop yield and water footprint assessment: Study of maize in the Po valley. Agricultural Systems 127, 139–149. doi:10.1016/j.agsy.2014.03.006

Neale, C.M.U., Bausch, W.C., Heermann, D.F., 1989. Development of reflectance-based crop coefficients for corn. Transactions of ASAE 32(6), 1891-1899. doi:10.13031/2013.31240

Pachepskya, Y., Acockb, B., 1998. Stochastic imaging of soil parameters to assess variability and uncertainty of crop yield estimates. Geoderma 85(2-3), 213-229.

Pereira, L.S., Allen, R.G., Smith, M., Raes, D., 2015. Crop evapotranspiration estimation with FAO56: Past

669 and future. Agricultural Water Management 147, 4–20. doi:10.1016/j.agwat.2014.07.031
670 Saadi, S., Simonneaux, V., Boulet, G., Raimbault, B., Mougenot, B., Fanise, P., Ayari, H., Lili-Chabaane, Z.,
671 2015. Monitoring Irrigation Consumption Using High Resolution NDVI Image Time Series: Calibration
672 and Validation in the Kairouan Plain (Tunisia). Remote Sensing 7, 13005–13028.
673 doi:10.3390/rs71013005
674 Smith, M., Allen, R.., Monteith, J.L., Perrier, A., Santos Pereira, L., Segeren, A., 1992. Expert Consultation
675 on Revision of FAO Methodologies for Crop Water Requirements. Presented at the Expert
676 Consultation on Revision of FAO Methodologies for Crop Water Requirements. Rome (Italy). 28-31
677 May 1990.
678 Steduto, P., Hsiao, T.C., Fereres, E., Raes, D., 2012. Crop yield response to water - FAO Irrigation and
679 drainage paper 66. FAO, Rome 505 pp.
680 Steduto, P., Hsiao, T.C., Raes, D., Fereres, E., 2009. AquaCrop—The FAO Crop Model to Simulate Yield
681 Response to Water: I. Concepts and Underlying Principles. Agronomy Journal 101, 426.
682 doi:10.2134/agronj2008.0139s
683 UNESCO, 2015. The United Nations world water development report 2015: water for a sustainable
684 world. UNESCO Publishing, Paris.
685 Toureiro, C., Serralheiro, R., Shahidian, S., Sousa, A., 2016. Irrigation management with remote sensing:
686 Evaluating irrigation requirement for maize under Mediterranean climate condition. Agricultural
687 Water Management.
688 Varlet-Grancher, C., Bonhomme, R., Chartier, M., Artis, P., 1982. Efficience de la conversion de l'energie
689 solaire par un couvert vegetal. Acta Oecologica Oecologia Plantarum 3, 3–26.
690 Vidal, J.-P., Martin, E., Franchistéguy, L., Baillon, M., Soubeyroux, J.-M., 2010. A 50-year high-resolution
691 atmospheric reanalysis over France with the Safran system. International Journal of Climatology 30,
692 1627–1644. doi:10.1002/joc.2003

693 Weiss, M., Baret, F., 1999. Evaluation of Canopy Biophysical Variable Retrieval Performances from the
694 Accumulation of Large Swath Satellite Data. Remote Sensing of Environment 70, 293-306. doi:
695 10.1016/S0034-4257(99)00045-0
696 Weiss, M., Baret, F., Leroy, M., Hautecœur, O., Bacour, C., Prévot, L., Bruguier, N., 2002. Validation of
697 neural net techniques to estimate canopy biophysical variables from remote sensing data.
698 Agronomie, 22, 547-553. doi:10.1051/agro:2002036
699 Zwart, S.J., Bastiaanssen, W.G.M., de Fraiture, C., Molden, D.J., 2010. WATPRO: A remote sensing based
700 model for mapping water productivity of wheat. Agricultural Water Management 97, 1628–1636.
701 doi:10.1016/j.agwat.2010.05.017